IOPscience iopscience.iop.org

Home Search Collections Journals About Contact us My IOPscience

Metal–insulator transitions in the half-filled ionic Hubbard model

This article has been downloaded from IOPscience. Please scroll down to see the full text article.

2010 J. Phys.: Condens. Matter 22 095602

(http://iopscience.iop.org/0953-8984/22/9/095602)

View the table of contents for this issue, or go to the journal homepage for more

Download details:
IP Address: 129.252.86.83
The article was downloaded on 30/05/2010 at 07:23

Please note that terms and conditions apply.

J. Phys.: Condens. Matter **22** (2010) 095602 (4pp) doi:10.1088/0953-8984/22/9/095602

Metal–insulator transitions in the half-filled ionic Hubbard model

A T Hoang

Asia Pacific Center for Theoretical Physics, POSTECH, San 31 Hyoja-dong, Pohang 790-784, Korea
and
Institute of Physics, PO Box 429, Bo Ho, Hanoi 10000, Vietnam

E-mail: hatuan@iop.vast.ac.vn

Received 18 August 2009, in final form 18 December 2009
Published 10 February 2010
Online at stacks.iop.org/JPhysCM/22/095602

Abstract

We study electronic phase transitions in the half-filled ionic Hubbard model with an on-site Coulomb repulsion U and an ionic energy Δ by using the coherent potential approximation. For a fixed and finite Δ two transitions from the band insulator via a metallic state to a Mott insulator are found with increasing U. The values of the critical correlation-driven metal–insulator transitions $U_{c1}(\Delta)$ and $U_{c2}(\Delta)$ are estimated. Our results are in reasonable agreement with the ones obtained by single-site dynamical mean-field theory and determinant quantum Monte Carlo simulation.

(Some figures in this article are in colour only in the electronic version)

1. Introduction

The ionic Hubbard model (IHM) was originally proposed to study the neutral–ionic transition in organic charge-transfer salts [1] or the ferroelectric transition in perovskite materials [2]. This model includes an on-site Coulomb repulsion (U) and a staggered potential that takes alternating values ($\pm\Delta$) on neighboring sites of a bipartite lattice. At half-filling, the ground state of the IHM is a band insulator (BI) for $\Delta \gg U$ and a Mott insulator (MI) for $U \gg \Delta$. It is natural to ask whether an intermediate phase can be found between the BI and MI phases. To answer this question, the IHM has been intensively studied both in low dimensions and in the limit of infinite dimension by a variety of techniques.

In one-dimensional (1D) IHM, many of the studies suggest that the direct transition from the BI to the MI is replaced by an intervening insulating bond-ordered phase [3–7]. The phase diagram of the IHM in 2D and at higher dimensions, however, is highly disputed. For 2D, the cluster dynamical mean-field theory (DMFT) [8] suggests a bond-ordered phase separating BI and MI regimes, while the determinant quantum Monte Carlo (DQMC) method [9] gives a metallic phase. At higher dimensions, on including antiferromagnetic long-range order, the Hartree–Fock theory [10] and the single-site DMFT [11] show that the system is insulating for all interaction strengths. On the other hand, within the single-site DMFT Garg *et al* [12] and Craco *et al* [13] have found that, if antiferromagnetism is suppressed due to frustration, then the intermediate phase between BI and MI is metallic, but it is unclear whether this metallic region shrinks to a line or if it ends up at a particular point by increasing the potential Δ. In addition, the nature of the phase transition between the metallic and the MI phases as well as between the BI and MI phases is still under debate. Generally, at present it is not clear which of the findings are due to the approximation used and which ones are independent of it.

The purpose of this paper is to study electronic phase transitions in the IHM at half-filling in two and three dimensions using the coherent potential approximation (CPA). This self-consistent approximation is known to be very successful in explaining single-particle properties of disordered systems and is well suited to study the Mott–Hubbard metal–insulator transition in the usual Hubbard model [14]. The CPA was also applied to intermediate-valence and heavy-fermion systems [15] as well as to study charge ordering in the extended Hubbard model [16].

2. Model and formalism

We consider the following Hamiltonian for the IHM on a bipartite lattice (sublattices A and B):

$$H = -t \sum_{i\in\mathrm{A}, j\in\mathrm{B},\sigma} [c^{\dagger}_{i\sigma} c_{j\sigma} + \mathrm{H.c.}] + U \sum_{i} n_{i\uparrow} n_{i\downarrow} + \varepsilon_{\mathrm{A}} \sum_{i\in\mathrm{A}} n_i + \varepsilon_{\mathrm{B}} \sum_{i\in\mathrm{B}} n_i - \mu \sum_{i} n_i, \quad (1)$$

 © 2010 IOP Publishing Ltd Printed in the UK

where $c_{i\sigma}(c^{\dagger}_{i\sigma})$ annihilates (creates) an electron with spin σ at site i, $n_{i\sigma} = c^{\dagger}_{i\sigma}c_{i\sigma}$ and $n_i = n_{i\uparrow} + n_{i\downarrow}$. t is the nearest-neighbor hopping parameter, U the on-site Coulomb repulsion, and $\varepsilon_{\rm A} = \Delta$ and $\varepsilon_{\rm B} = -\Delta$ the ionic energies. The chemical potential is chosen to be $\mu = U/2$, so that the average occupancy is 1 (half-filling).

In the alloy-analog approach the many-body Hamiltonian (1) is replaced by a one-particle Hamiltonian with disorder which is of the form

$$H = \sum_{i\in{\rm A},\sigma} E_{{\rm A}\sigma} n_{i\sigma} + \sum_{i\in{\rm B},\sigma} E_{{\rm B}\sigma} n_{i\sigma} - t \sum_{i\in{\rm A},\, j\in{\rm B},\sigma} [c^{\dagger}_{i\sigma}c_{j\sigma} + {\rm H.c.}], \tag{2}$$

where

$$E_{\alpha,\sigma} = \begin{cases} \varepsilon_\alpha - U/2 & \text{with probability } 1 - n_{\alpha,-\sigma}, \\ \varepsilon_\alpha + U/2 & \text{with probability } n_{\alpha,-\sigma}. \end{cases} \tag{3}$$

Here $\alpha = {\rm A}, {\rm B}$ and $n_{\alpha,\sigma}$ is the average occupation with spin σ in the α-sublattice. As in [12, 13] we focus in this paper on the paramagnetic case, for which $n_{\alpha\uparrow} = n_{\alpha\downarrow} = n_\alpha/2$. The Green function corresponding to the Hamiltonian (2) has to be averaged over all possible configurations of the random potential which can be considered to be due to alloy constituents. The averaging cannot be performed exactly. To solve the alloy problem the CPA is used. In such an approximation the averaged local Green function for the α-sublattice $G_\alpha(\omega)$ takes the form [16]

$$G_\alpha(\omega) = \frac{2}{W^2}\left\{\omega - \Sigma_{\bar\alpha} - \left[(\omega - \Sigma_{\bar\alpha})^2 - \frac{\omega - \Sigma_{\bar\alpha}}{\omega - \Sigma_\alpha} W^2\right]^{1/2}\right\}, \tag{4}$$

with $\alpha = {\rm A(B)}$ and $\bar\alpha = {\rm B(A)}$, where $\Sigma_\alpha \equiv \Sigma_\alpha(\omega)$ is the self-energy for the α-sublattice. Here we have employed the semi-elliptic density of states (DOS) for non-interacting electrons, $\rho_0(\omega) = \frac{2}{\pi W^2}\sqrt{W^2 - \omega^2}$, W is the half-width of the band, which sets the energy unit. Note that this model DOS is often used as an additional approximation in combination with the CPA. As was noted in [17], for the Bethe lattice of connectivity $z \geqslant 3$ this approximation is good, at least in a qualitative sense. Therefore, it is reasonable to believe our calculation is applicable to the IHM in dimensions $D \geqslant 2$. The CPA demands that the scattering matrix vanishes on average. This yields an expression for $\Sigma_\alpha(\omega)$ of the form

$$\Sigma_\alpha = \bar E_\alpha - (\varepsilon_\alpha - U/2 - \Sigma_\alpha) G_\alpha(\omega)(\varepsilon_\alpha + U/2 - \Sigma_\alpha), \tag{5}$$

where $\bar E_\alpha = \varepsilon_\alpha + U(n_\alpha - 1)/2$. Eliminating $\Sigma_\alpha(\omega)$ from (4) and (5) leads to a pair of equations for $G_{\rm A}(\omega)$ and $G_{\rm B}(\omega)$:

$$\begin{aligned} &\tfrac{1}{16} G^2_{\bar\alpha}(\omega) G_\alpha(\omega) - \tfrac{1}{2}(\varepsilon_\alpha - \omega) G_{\bar\alpha}(\omega) G_\alpha(\omega) \\ &\quad + \left[(\varepsilon_\alpha - \omega)^2 - \frac{U^2}{4}\right] G_\alpha(\omega) - \frac{1}{4} G_{\bar\alpha}(\omega) \\ &\quad + \varepsilon_\alpha - \omega - \frac{U}{2}(n_\alpha - 1) = 0. \end{aligned} \tag{6}$$

Equation (6) must now be solved with $n_{\rm A} + n_{\rm B} = 2$, where $n_\alpha = -2/\pi \int_{-\infty}^{0} {\rm Im}\, G_\alpha(\omega)\, {\rm d}\omega$. From the self-consistent CPA solution of the IHM one can determine the local one-particle DOS $\rho_\alpha(\omega) = -{\rm Im}\, G_\alpha(\omega)/\pi$, the staggered charge density $n_{\rm B} - n_{\rm A}$ and the charge gap as functions of the model parameters U and Δ. A metal is distinguished from an insulator by a finite total DOS at the Fermi level, i.e. $\rho(0) = \sum_\alpha \rho_\alpha(0) > 0$.

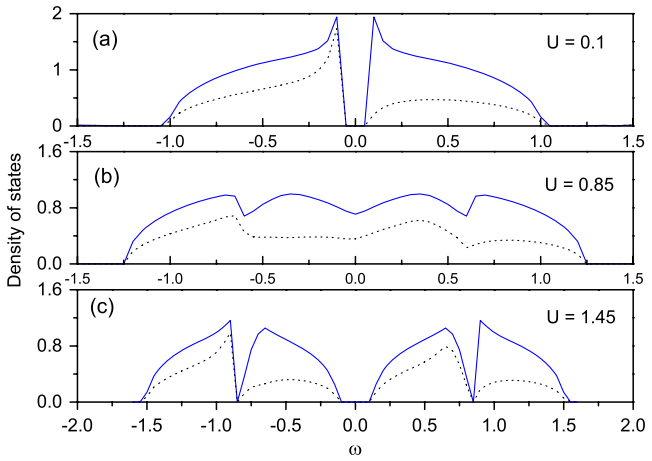

Figure 1. Total and local DOS for B-sublattice for $\Delta = 0.1$ and different values of U. DOS exhibits gaps for $U = 0.1$ (a) and 1.45 (c), corresponding to band and Mott insulating states, respectively. Energy scale: $W = 1$. (a) Band insulator; (b) metal and (c) Mott insulator.

3. Results and discussion

Before numerically solving equation (6), let us briefly consider limiting cases. In the absence of a staggered potential, setting $\Delta = 0$ in (6) we reproduce the CPA equation for the Green function obtained by Velicky *et al* in the usual Hubbard model [18]. The critical Coulomb repulsion for the Mott–Hubbard metal–insulator is found to be $U_{\rm c} = W = 1$. In the non-interacting ($U = 0$) limit within the CPA the system is a band insulator with the exact charge gap 2Δ.

We turn now to present our numerical results. Figure 1 shows the total and local DOS for the B-sublattice for $\Delta = 0.1$ and for three values of U corresponding to the three different phases. The solid and the dotted lines correspond to the total and the local DOS, respectively. For $U = 0.1$ and 1.45, corresponding to the BI and MI phases, the DOS shows a gap around $\omega = 0$, indicating an insulator. Additionally, at small U the gap is small, of the order of Δ; at large U in addition to the gap around $\omega = 0$ we also found two small gaps around $\omega \approx \pm 0.85$. The latter reflects a band splitting due to alloy disorder, as was noted in [19, 20]. In contrast, the DOS at the Fermi level for $U = 0.85$ is nonzero, which indicates a metallic phase. Here, as in [13, 19], the imaginary part of $\Sigma_\alpha(\omega)$ (not shown) is finite at the Fermi level. Similar behaviors of the DOS were also found in the DMFT and DQMC studies of this system [9, 11–13].

The power of the CPA lies in its simplicity. Since $\rho_{\rm A}(\omega) = \rho_{\rm B}(-\omega)$ is valid at half-filling, it follows that $\rho_{\rm A}(0) = \rho_{\rm B}(0)$. Then from equation (6) it can be verified that for fixed Δ the necessary conditions for $\rho(0) \neq 0$, i.e. the system is metallic, are $2\Delta < U(\Delta) < \sqrt{4\Delta^2 + 1}$. In other words, within the CPA the metallic phase of the system

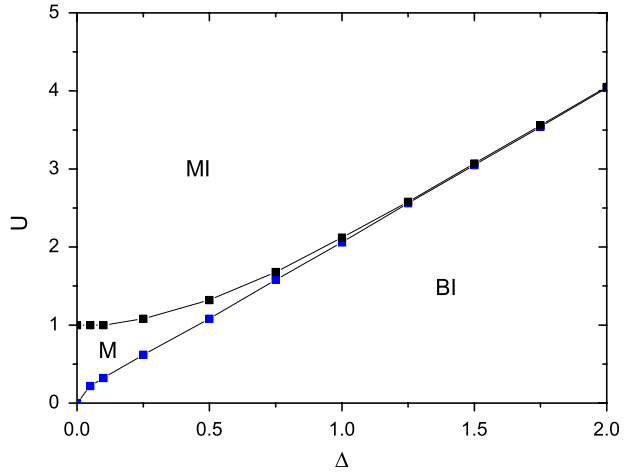

Figure 2. The $T = 0$ phase diagram of the IHM obtained by the CPA in combination with the semi-elliptical model DOS. The upper phase boundary $U_{c2}(\Delta)$ approximately equals $\sqrt{4\Delta^2 + 1}$, whereas for $\Delta \geqslant 0.5$ the lower one is almost identical to the strong coupling boundary line $U = 2\Delta$.

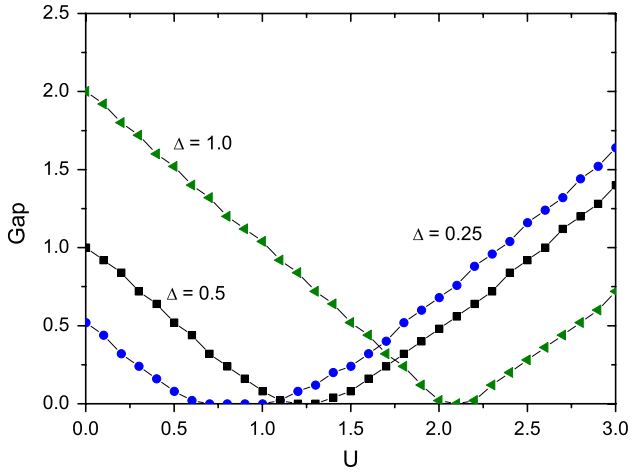

Figure 3. Charge gap of the IHM as a function of U for different values of Δ.

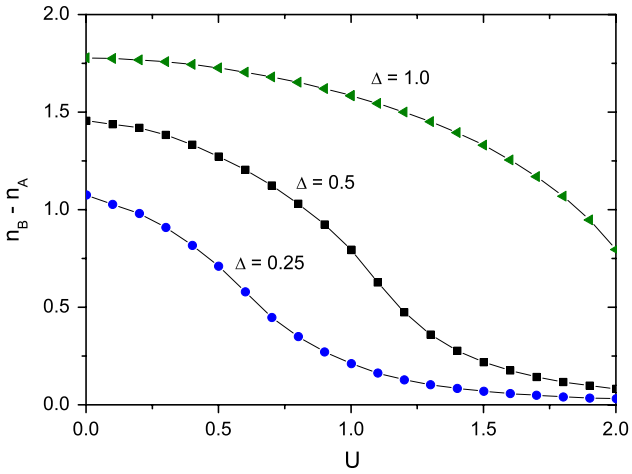

Figure 4. Staggered charge density $n_B - n_A$ as a function of U for different values of Δ. Our results for $\Delta = 0.5$ and 1.0 are in good agreement with those obtained within single-site DMFT in [11]. In the CPA the phase transitions are clearly continuous.

is sandwiched between $U_{c1}(\Delta)$ and $U_{c2}(\Delta)$, where $2\Delta < U_{c1}(\Delta) < U_{c2}(\Delta) < \sqrt{4\Delta^2 + 1}$. Consequently, the metallic region becomes vanishing small for $\Delta \gg 1$ and approaches the strong coupling boundary line $U = 2\Delta$ when $\Delta \to \infty$. It means that the CPA nicely reproduces the phase diagram in the atomic limit ($t = 0$). In figure 2 we present the obtained phase diagram for the half-filling IHM. It is interesting to compare our phase diagram with the ones derived by DQMC and DMFT of the IHM in two and higher dimensions. In agreement with the single-site DMFT results [12, 13] we find the metallic phase along the $\Delta = 0$ axis, and as the cluster DMFT [8] and the DQMC [9] our intermediate phase is located slightly above the line $U = 2\Delta$. The shape of our metallic region is similar to the ones obtained in [13], which are considerably enlarged in comparison with those in [12], keeping in mind that in [12, 13] $2t = W$. However, the CPA does not allow us to determine the coexistence region between metal and MI or between BI and MI as in [13]. Additionally, our results support the view that the metallic phase shrinks to a line by increasing the ionic energy Δ. The charge gap as a function of U for three values of Δ is plotted in figure 3. For $U < U_{c1}(\Delta)$ our results are compatible with those obtained in [13] and we find the system is a band insulator with a gap of the order of $(2\Delta - U)$. The gap is suppressed to zero at $U = U_{c1}(\Delta)$ and remains zero within the metallic phase when $U_{c1}(\Delta) \leqslant U \leqslant U_{c2}(\Delta)$. For $U = U_{c2}(\Delta)$ there is a second transition from the metal to a Mott insulator, in which the gap is of the order of $(U - \sqrt{4\Delta^2 + 1})$. In figure 4 we show the CPA result for the staggered charge density $n_B - n_A$ as a function of U for different values of Δ. For fixed Δ the charge density decreases with increasing U and approaches zero for large U. Our results for $\Delta = 0.5$ and 1.0 are in good agreement with those obtained within single-site DMFT in [11], keeping in mind that in [11] the bandwidth sets the energy unit. As in DQMC work [9], in the CPA the phase transitions are clearly continuous, in contrast to the results in [8, 13], where DMFT studies give a first-order transition between the intermediate phase and the Mott insulator.

4. Conclusions

We have applied the CPA to study electronic phase transitions in the half-filled IHM in dimensions $D \geqslant 2$. We derive the U–Δ phase diagram which well recovers the limiting cases and is in reasonable agreement with the ones obtained by single-site DMFT and DQMC simulation. We find also continuous phase transitions between the metallic and insulating phases.

As in the DMFT, in the limit $D \to \infty$ the CPA yields exact results for one-particle properties. In studying the electronic boundary phase in the IHM the CPA has advantages over the DMFT and DQMC of being analytically simple. It provides some analytical results and does not require much computer work. Although the CPA is unable to capture nonlocal correlations and is more accurate at high temperatures, comparing our results with the ones obtained by DMFT and DQMC methods, we believe that the CPA can still catch the essential physics of the system in the paramagnetic

sector at low temperatures, and therefore it gives a correct qualitative picture of the metal–insulator transitions in the IHM. Based on the CPA results as well as the ones obtained by single-site DMFT and DQMC in previous studies we may speculate that the presence of a metallic phase intervening between the band and Mott insulating phases in the half-filled IHM at high dimensions is not an issue of the approximation, but a real feature of the system. We expect that, in the near future, by using optical lattices the physics of the IHM can be realized in experimental practice.

The calculations presented here can be extended to the IHM away from half-filling and/or at finite temperature. Within the CPA one can also evaluate the temperature dependence of the conductivity for a wide range of model parameters and then calculate the electronic phase diagram of the system. However, to obtain the precise nature of the transitions and the intervening phases further investigations by more sophisticated methods are required. This is left to future work.

Acknowledgments

This work was done during a visit by the author to the Asia Pacific Center for Theoretical Physics, whose hospitality and support are gratefully acknowledged. The author also acknowledges the Department of Physics, POSTECH for sharing CPU time. Thanks are due to Professor P Fulde and Dr M T Tran for useful discussions and the National Foundation of Science and Technology Development (NAFOSTED) for support.

References

[1] Hubbard J and Torrance J B 1981 *Phys. Rev. Lett.* **47** 1750
[2] Egami T, Ishihara S and Tachiki M 1993 *Science* **261** 1307
[3] Fabrizio M, Gogolin A O and Nersesyan A A 1999 *Phys. Rev. Lett.* **83** 2014
[4] Winkens T and Martin R M 2001 *Phys. Rev.* B **63** 235108
[5] Batista C D and Aligia A A 2004 *Phys. Rev. Lett.* **92** 246405
[6] Manmana S R *et al* 2004 *Phys. Rev.* B **70** 155115
[7] Fehske H, Hager G and Jeckemann J 2008 *Europhys. Lett.* **84** 57001
[8] Kancharla S S and Dagotto E 2007 *Phys. Rev. Lett.* **98** 016402
[9] Bouadim K *et al* 2007 *Phys. Rev.* B **76** 085112
[10] Pozgajcic K and Gros C 2003 *Phys. Rev.* B **68** 085106
[11] Byczuk K *et al* 2009 *Phys. Rev.* B **79** 121103 (R)
[12] Garg A, Krishnamurthy H R and Randeria M 2006 *Phys. Rev. Lett.* **97** 046403
[13] Craco L *et al* 2008 *Phys. Rev.* B **78** 075121
[14] Gebhard F 1997 *The Mott Metal–Insulator Transition: Models and Methods* (New York: Springer)
[15] Czycholl G 1986 *Phys. Rep.* **143** 277
[16] Hoang A T and Thalmeier P 2002 *J. Phys.: Condens. Matter* **14** 6639
[17] Vlaming R and Vollhardt D 1992 *Phys. Rev.* B **45** 4637
[18] Velicky B, Kirkpatrick S and Ehrenreich H 1968 *Phys. Rev.* **175** 747
[19] Byczuk K *et al* 2004 *Phys. Rev.* B **69** 045112
[20] Balzer M and Potthoff M 2005 *Physica* B **359–361** 768